

## Supporting Information

### S1 Materials

Toluene (Thermo Fischer), propylene carbonate (Sigma Aldrich), 3-(Trimethoxysilyl) propyl methacrylate (Sigma Aldrich), pentaerythritol triacrylate (PETA, Sigma Aldrich), poly(ethylene glycol) diacrylate (PEG-DA,  $M_n = 700 \text{ g mol}^{-1}$ , Sigma Aldrich), 2-Benzyl-2-dimethylamino-1-(4-morpholinophenyl)-butanone (Irgacure 369, Sigma Aldrich), Rhodamine B (Sigma Aldrich) and poly(ethylene glycol) methyl ether acrylate (PEGMEA, Sigma Aldrich) were used as received.

### S2 Instrumentation

Direct laser writing was performed with a NanoScribe Photonic Professional GT. All structures were printed in oil-immersion mode using a 63× oil immersion objective (NA=1.4).

Fluorescence intensities of microstructures were measured using a Nikon A1R confocal laser scanning microscope. An excitation wavelength of 405 nm was employed and the emitted fluorescence between 425 nm and 475 nm was detected. The fluorescence of each individual microstructure was measured over the course of one minute and averaged over time and over all microstructures. Measurements were taken at five different z heights each and the height with the greatest fluorescence was chosen for each block to ensure the measurements would be consistent even though the blocks have different heights. The imaging parameters (e.g. laser power, gain, and aperture) were kept the same between measurements, so as to allow relative quantification.

Images of fluorescent microstructures were recorded using a Leica SP8 confocal laser scanning microscope. The anthracene fluorescence was excited at 405 nm and detected between 410 nm and 520 nm. The rhodamine B fluorescence was excited at 573 nm and detected between 578 nm and 700 nm.

Scanning electron microscopy images were captured using a Zeiss Sigma VP Field emission SEM at 10 kV using a secondary electron detector. Samples were coated with a 2 nm layer of platinum.

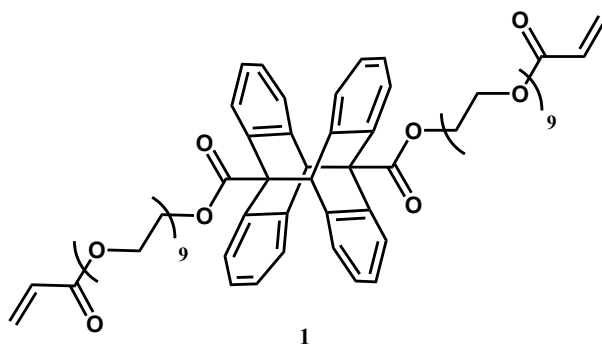
NanoDMA measurements were performed using a Hysitron TI950 Nanoindenter equipped with a nanoDMA III transducer. A tip with the Berkovich geometry was used to perform all measurements. Analysis of the microstructure samples was conducted as follows: After every irradiation step, three of the blocks were analysed. They were subjected to a quasistatic force of 200  $\mu\text{N}$ , modulated by an oscillatory force of 10  $\mu\text{N}$ . For the results presented herein, the oscillatory force was applied with a frequency of around 200 Hz. The results of the three blocks analysed after each irradiation step were averaged, to account for possible variation between the structures.

ToF-SIMS data were acquired using an IONTOF M6 instrument (IONTOF GmbH, Münster, Germany) equipped with a reflectron time-of-flight analyser and Bi/Mn primary-ion source.  $\text{Bi}_3^+$  cluster ions were selected from the pulsed primary-ion beam for the analysis. In order to attain the sub-micron spatial resolution required to image the scaffolds, whilst also maintaining good mass resolution ( $m/\Delta m > 5000$ ), pulses were 'unbunched' and the analyser operated in delayed-extraction mode.<sup>1</sup> Primary-ion doses were limited to  $10^{-11} \text{ ions cm}^{-2}$ , which is well below the static limit; however, it was observed during the initial analyses that both the scaffolds and substrate were coated with unreacted material, much of which was removed by sputtering for a few seconds with a 2.5 keV  $\text{Ar}_{800}$  gas-cluster

ion beam. In images acquired after this 'cleaning' step, the association of several secondary ions with sub-structures of the sample was more apparent.

To compensate for surface charging, the sample was flooded with low-energy (21 eV) electrons between primary-ion pulses. Spectra were acquired in positive polarity, and the mass scale calibrated using peaks attributed to hydrocarbon ions ( $C_2H_3^+$ ,  $C_3H_3^+$ ,  $C_4H_3^+$ ,  $C_5H_3^+$ ,  $C_6H_3^+$ ). During data acquisition, the pressure in the analysis chamber was maintained at, or below,  $1 \times 10^{-8}$  mbar.

### S3 Synthesis



**Scheme S1:** Synthesis of the anthracene dimer **1**.

For the full synthesis procedure, please refer to our previous publication.<sup>2</sup>

## S4 Direct Laser Writing

Before writing, all cover slip glass substrates were functionalized with 3-(Trimethoxysilyl)propyl methacrylate. This was done by plasma cleaning the substrates for 15 min to activate them, before immersing them in a 5mM solution in toluene for 60 min. The functionalized substrates were then rinsed with toluene, acetone and water.

Microstructures written from three different resist compositions are presented herein:

**Table S1:** Compositions of the photoresists used to write structures presented herein. All values given in wt%. All propylene carbonate is assumed to have been washed out through the described washing procedure. All acrylate species are assumed to react with equal efficiency, leading to the given ratios in the structures.

|   | Photo-responsive resist 1 |            | Photo-responsive resist 2 |            | Photo-responsive resist 3 |            |
|---|---------------------------|------------|---------------------------|------------|---------------------------|------------|
|   | Resist                    | Structures | Resist                    | Structures | Resist                    | Structures |
| Anthracene dimer 1                      | 72                        | 90         | 76                        | 95         | 78                        | 97.5       |
| PETA                                    | 6                         | 7.5        | 2                         | 2.5        | 0                         | 0          |
| PEG-DA ( $M_n=700 \text{ g mol}^{-1}$ ) | 0                         | 0          | 0                         | 0          | 0                         | 0          |
| Irgacure 369                            | 2                         | 2.5        | 2                         | 2.5        | 2                         | 2.5        |
| Rhodamine B                             | 0                         | 0          | 0                         | 0          | 0                         | 0          |
| Propylene carbonate                     | 20                        | 0          | 20                        | 0          | 20                        | 0          |
|   | Fluorescent resist 4      |            | Blank resist 5            |            |                           |            |
|   | Resist                    | Structures | Resist                    | Structures |                           |            |
| Anthracene dimer 1                      | 0                         | 0          | 0                         | 0          |                           |            |
| PETA                                    | 77                        | 96.5       | 6                         | 7.5        |                           |            |
| PEG-DA ( $M_n=700 \text{ g mol}^{-1}$ ) | 0                         | 0          | 72                        | 90         |                           |            |
| Irgacure 369                            | 2                         | 2.5        | 2                         | 2.5        |                           |            |
| Rhodamine B                             | 1                         | 1          | 0                         | 0          |                           |            |
| Propylene carbonate                     | 20                        | 0          | 20                        | 0          |                           |            |

The block microstructures were written from the photo-responsive resist **1**, as well as from the blank resist **5**, with laser powers ranging between 6 mW and 14 mW. The scan speed was varied between 200  $\mu\text{m/s}$  and 5000  $\mu\text{m/s}$ .

The boxing ring structures were written in two steps. In the first step, the frames were written from commercial IP-S resist (laser power=16 mW, scan speed=3000  $\mu\text{m/s}$ ). For the frames that were used to record CLSM images, the fluorescent resist 2 was used instead. After the first writing step, the samples were developed in the way described below. In a second step, the bridges between the frames were written from the photo-responsive resist **1** and developed in the same way afterwards.

After writing, all samples were developed by immersing the cover slips in poly(ethylene glycol) methyl ether acrylate (PEGMEA) for at least 10 min and then washed by immersing them in isopropyl alcohol for at least 5 min.

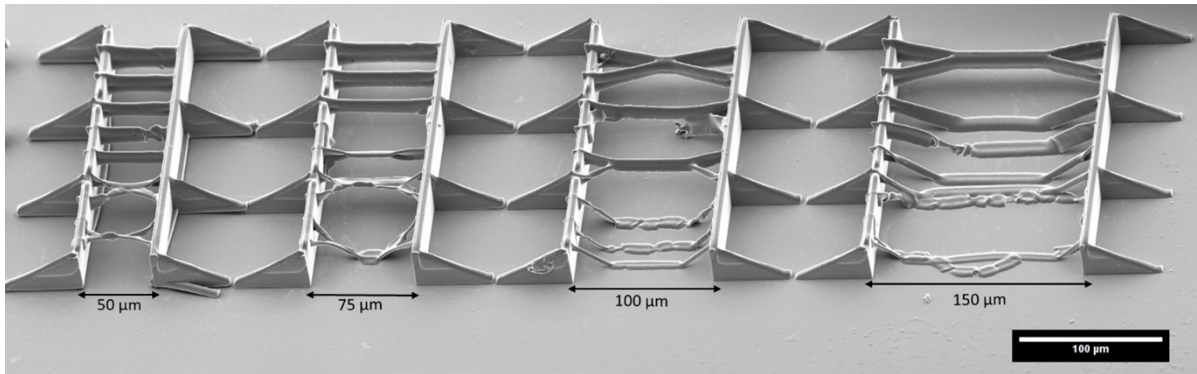


**Fig. S 1:** Bridges of different dimensions printed from photo-responsive resist **3** in between frames of IP-S.

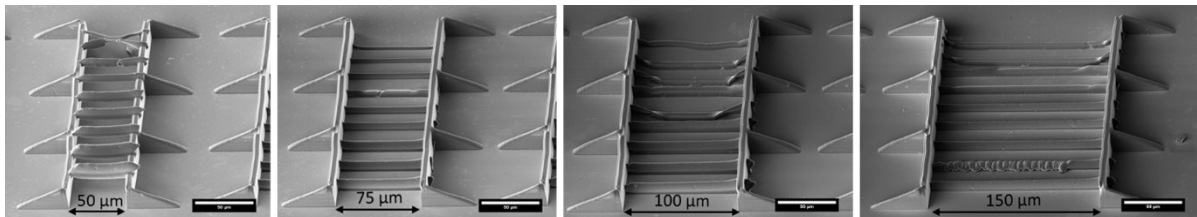


**Fig. S 2:** Bridges of different dimensions printed from photo-responsive resist **2** in between frames of IP-S. All scale bars: 50 μm

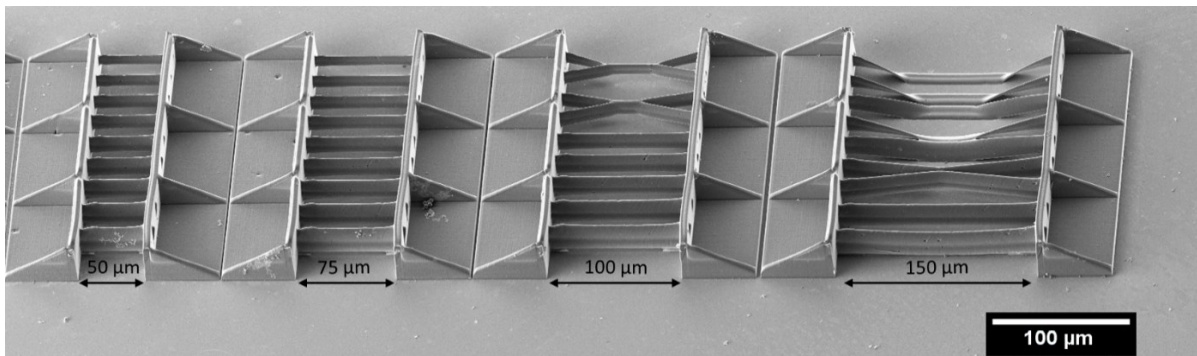


**Fig. S 3** Bridges of different dimensions printed from photo-responsive resist **1** in between frames of IP-S.

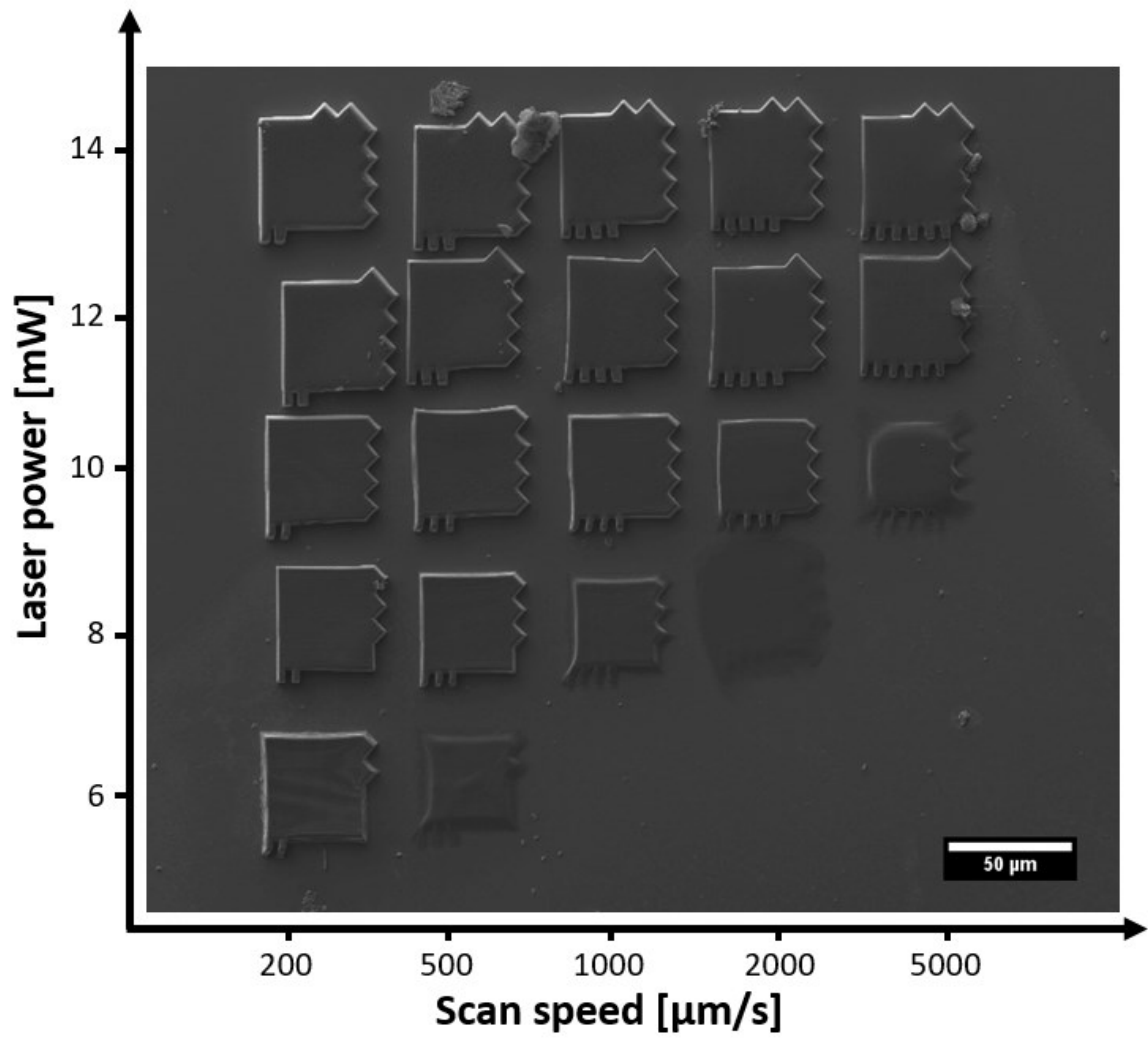
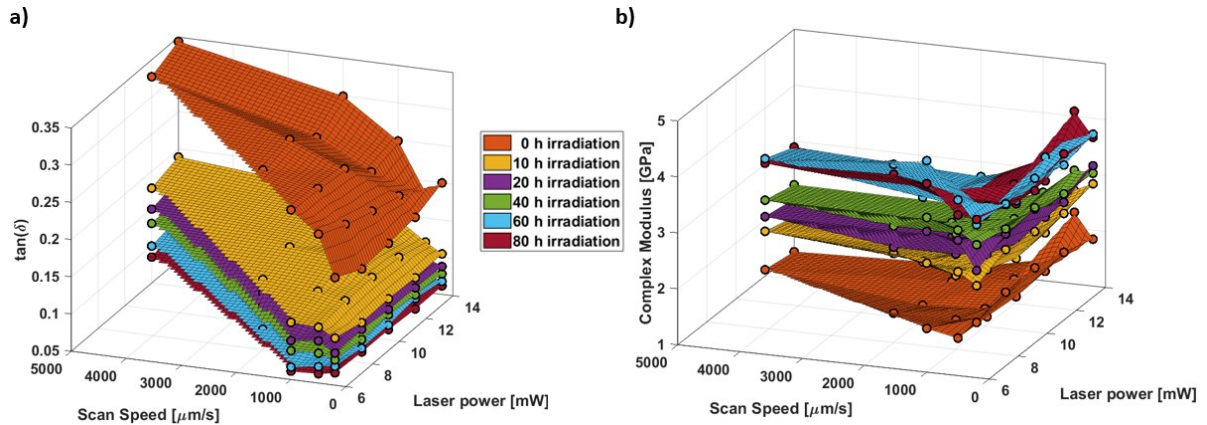


Fig. S 4: SEM image of microstructures written from blank resist 5.

## S5 Measurements of mechanical properties

For a full consideration of the theory behind the measurements of the mechanical measurements, please refer to our previous publication.<sup>2</sup>



**Fig. S 5:** Additional measurements of the mechanical properties of the photo-responsive microstructures over the course of irradiation. a) Loss factor. b) Complex modulus.

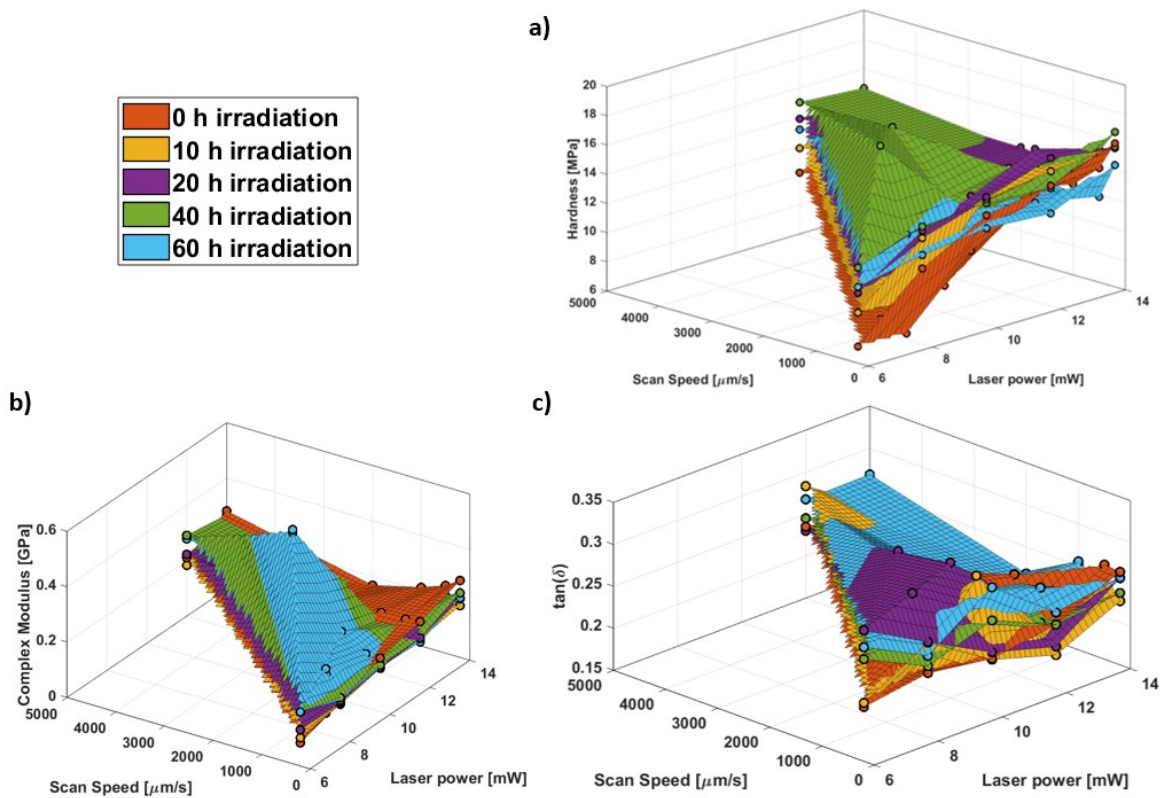


**Fig. S 6:** Full mechanical measurements of the blank microstructures. a) Hardness. b) Complex modulus. c) Loss factor.

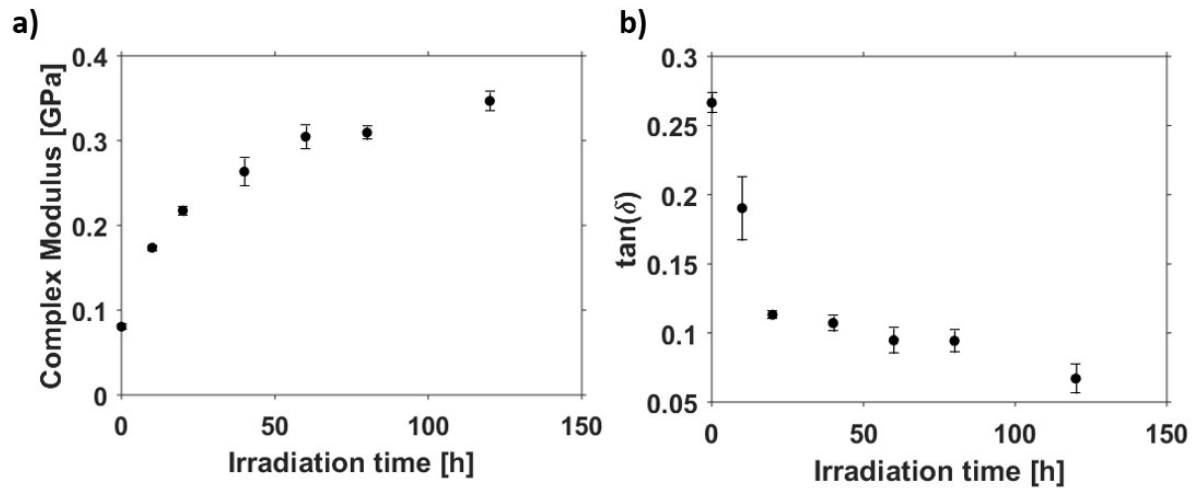


**Fig. S 7:** Additional measurements of the mechanical properties of the photo-responsive bridges of the multi-material boxing ring microstructures over the course of irradiation. a) Complex modulus. b) Loss factor.

## S6 ToF-SIMS

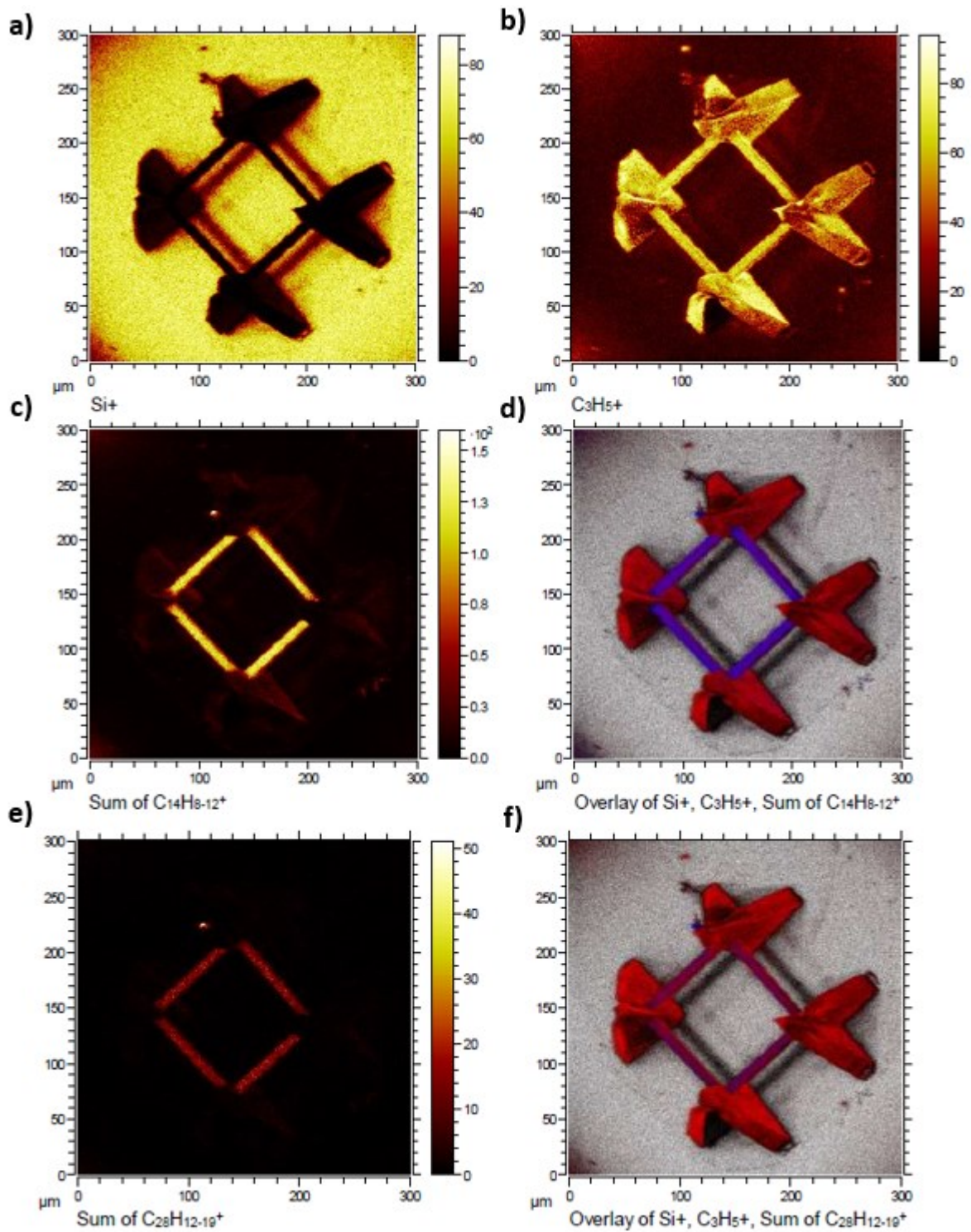


**Fig. S 8:** Additional ToF-SIMS ion maps. a)  $\text{Si}^+$ . b)  $\text{C}_3\text{H}_5^+$ . c)  $\text{C}_{14}\text{H}_8\text{-}_{12}^+$ . d) Sum of  $\text{Si}^+$  (grey),  $\text{C}_3\text{H}_5^+$  (red) and  $\text{C}_{14}\text{H}_8\text{-}_{12}^+$  (blue). e)  $\text{C}_{28}\text{H}_{12}\text{-}_{19}^+$ . f) Sum of  $\text{Si}^+$  (grey),  $\text{C}_3\text{H}_5^+$  (red) and  $\text{C}_{28}\text{H}_{12}\text{-}_{19}^+$  (blue).



1. T. K. Claus, B. Richter, V. Hahn, A. Welle, S. Kayser, M. Wegener, M. Bastmeyer, G. Delaittre and C. Barner-Kowollik, *Angewandte Chemie International Edition*, 2016, **55**, 3817-3822.
2. M. Gernhardt, E. Blasco, M. Hippler, J. Blinco, M. Bastmeyer, M. Wegener, H. Frisch and C. Barner-Kowollik, *Adv. Mater.*, 2019, **31**, 1901269.